Structure of Short DNA Fragment Solutions

J. R. C. van der Maarel* and K. Kassapidou

Leiden Institute of Chemistry, Gorlaeus Laboratories, Leiden University, P.O. Box 9502, 2300 RA Leiden, The Netherlands

Received April 14, 1998; Revised Manuscript Received July 6, 1998

ABSTRACT: The structure function of DNA fragments (contour length 54−104 nm) immersed in aqueous salt solutions is determined with small angle neutron scattering. From the limiting behavior at high values of momentum transfer an effective diameter or second moment of the DNA cross section of 1.6 nm is derived. For low values of momentum transfer and/or high ionic strength, the effects of supporting electrolyte, DNA concentration, and DNA contour length can be rationalized with virial theory including screened electrostatics. With excess monovalent salt concentration exceeding, e.g., 1 M, neutral polymer behavior is recovered.

Introduction

DNA is a highly charged polymer and the distribution of segments, counterions, and possibly added low molecular weight salt is a problem of general interest related to effects of long-range Coulomb interaction. Due to strong charge coupling, small ions accumulate about DNA and a double layer is formed. The double layer has important consequences for, e.g., thermodynamic properties and inter- and intramolecular polyelectrolyte organization.[1−3] An illustrative example of the latter category is the effects of charge and supporting electrolyte concentration on the formation of DNA liquid crystals.[4−6] With small angle neutron scattering (SANS) and contrast variation in the water we obtained information about the double layer without resorting to a model describing chain correlations.[7−9] As in case of many thermodynamic data, these structural results agree with correlation functions obtained from the solution of the (nonlinear) Poisson−Boltzmann equation.

Despite many experimental and theoretical efforts, little is known about the effect of charge on interchain correlations. Especially, for highly charged polymers such as DNA, nonlinear screening effects are important. These effects are often accounted for by renormalization of the polyion charge and electrostatic interactions are evaluated in the Debye−Hückel approximation (i.e., the potential is obtained from the solution of the linearized Poisson−Boltzmann equation).[10,11] The introduction of *effective* charges and the use of *screened* electrostatics are relevant for properties that are most sensitive to interactions beyond the inner double layers. Especially, the virial coefficients in the solution free energy expansion can be calculated to high accuracy, because of unfavorable Boltzmann weighing of configurations with interaction energies exceeding thermal energy kT.[12] For rodlike polyelectrolytes, the structure function has been solved with virial theory and screened electrostatic interactions.[13−15] The theoretical prediction compares favorably with the structure factor of charged rodlike TMV and fd virus solutions in the presence of excess simple salt.[16] However, virial theory is strictly applicable for wavelengths exceeding the screening length and cannot be used to predict structural order on a distance scale on the order of the inverse double layer thickness.

For short persistence length DNA fragments, the calculated virial coefficients compare reasonably well with experimental values obtained from static laser light scattering in the long wavelength limit ($qL < 1.8$ and at zero angle).[17,18] In ref 18 it was shown that the virial expansion has to be carried up to and including the third coefficient. Furthermore, at a certain critical concentration, which increases with increasing added salt concentration, the DNA fragments form loose aggregates. For similar fragments, Wang and Bloomfield reported the structure function for higher values of momentum transfer from small angle X-ray scattering.[19] In particular, these authors reported the scaling of the correlation peak with DNA volume fraction and/or supporting electrolyte concentration.

For short fragments immersed in salt solutions we determined the DNA structure function with SANS. The most probable contour length is 54 or 104 nm, which is approximately 1 or 2 times, respectively, the persistence length (50 nm). The DNA concentration is below the critical concentration for the onset of the formation of aggregates.[18] Within the present range of momentum transfer ($qL > 5$) the intrachain structure can to a good approximation be described by the high q limiting form of the form function of a rod with a finite cross section. The cross section is obtained from a fit in the presence of excess salt to suppress intermolecular interference. Effects of intermolecular organization are most clearly demonstrated when the total static structure function is divided by the intrachain form function. It will be shown that for low q values and/or high supporting electrolyte concentration the scattering behavior agrees with virial theory and screened electrostatics. In particular, for strongly interacting systems at low ionic strength, significant deviations are observed when the momentum transfer is on the order of the inverse double layer thickness.

Theory

In the present solutions the scattering is dominated by the DNA polyion structure, because the nucleotide scattering length contrast exceeds the corresponding

* Author for correspondence.

S0024-9297(98)00571-3 CCC: $15.00
Published on Web 08/05/1998

values of the small ions by 2 orders of magnitude. The coherent part of the solvent-subtracted SANS intensity reads

$$I(q)/\rho = \bar{b}^2 S(q) \tag{1}$$

with ρ the DNA concentration in number of nucleotide monomers per unit volume, $\bar{b}$ the scattering length contrast, and q denoting momentum transfer. The static structure function $S(q)$ is the spatial Fourier transform of the nucleotide density correlation function[20]

$$S(q) = \frac{1}{\rho V}\int_V \mathrm{d}\vec{r}\; e^{-i\vec{q}\cdot\vec{r}}\langle\rho(0)\rho(\vec{r})\rangle \tag{2}$$

and can be expressed as a sum of an intra- $F(q)$ and an intermolecular $H^{II}(q)$ part:

$$S(q) = F(q) + \rho\, H^{II}(q) \tag{3}$$

The solution structure is often defined by the ratio of the total static structure function and the intrachain part $S(q)/F(q)$. For asymmetric particles the solution structure function does not contain information about the center of mass distribution only, but is also sensitive to coupling between orientation and translation degrees of freedom. As q is increased, $H^{II}(q)$ becomes progressively less important and the solution structure approaches unity.

For monodisperse fragments the intrachain function $F(q)$ is related to the form function $P(q)$ (normalized to unity at $q = 0$) according to $F(q) = N\,P(q)$, with N the number of nucleotides per fragment. The DNA molecules can be considered as semiflexible wormlike chains with persistence length $L_p \approx 50$ nm and the most probable contour length L amounts 54 or 104 nm (see Table 1). Our experiments are done at relatively high values of momentum transfer, i.e., $qL \gg 1$ with a lower bound $qL \approx 5$. With $L \lesssim 2\,L_p$ and $qL \gg 1$, flexibility and finite length effects are negligible and $F(q)$ takes to a good approximation the limiting form[8,21]

$$F(q) = \frac{\pi}{qA}[a(q)]^2, \quad qL \gg 1 \tag{4}$$

with $A = L/N$ the z-axis projected distance between nucleotides (0.171 nm). In eq 4 the term $a(q)$ denotes the Hankel transform of the radial density profile of the DNA cross section. If the radial density is assumed to be uniform for $0 \le r \le r_p$ and given by $\rho(r)A\pi\, r_p^2 = 1$ and zero for $r > r_p$, with r_p being the DNA radius, one obtains[7]

$$a(q) = \frac{2J_1(qr_p)}{qr_p} \tag{5}$$

with J_1 the first order Bessel function of the first kind. The DNA cross section becomes progressively more important for higher values of momentum transfer (in the range $qr_p \approx 1$) and is responsible for a deviation from rodlike q^{-1} scaling. For the full expression of the rod form function including finite length effects, the reader is referred to refs 7 and 8.

For rodlike polyelectrolytes, the structure function has been solved with virial theory and electrostatic interactions in the Debye−Hückel approximation. In case of uncharged rods in the second virial approximation Shimada *et al.* derived the basic integral equation via linear response.[22] Van der Schoot and Odijk proposed a solution using a variation approach, which agrees well with numerical work by Maeda.[23,24] Electrostatic interactions were included in the variation procedure by Maeda and Odijk.[13,14] Odijk carried the virial expansion up to and including the third virial coefficient.[15] In the high q asymptotic limit ($qL \gg 1$), the structure function takes the form[15]

$$\frac{1}{S} = \left[\frac{qL}{\pi} + \frac{2}{\pi^2} + \frac{16A_2\rho_L}{\pi^2} + 3A_3\,\rho_L{}^2 + O\left(\frac{1}{qL}\right)\right]\frac{1}{N[a(q)]^2} \tag{6}$$

with $\rho_L = \rho/N$ being the rod number concentration and A_2 and A_3 denoting the second and third virial coefficient, respectively. The structure function has been corrected for the finite DNA cross section by multiplication with the squared radial Hankel transform $a(q)$.

The virial coefficients are calculated on the basis of the assumption that the excluded volume can be viewed as a sum of a hard core and an electrostatic part. Configurations with interaction energies exceeding kT are exceptional, because of unfavorable Boltzmann weighing. Accordingly, for the evaluation of the electrostatic contribution, the particles are replaced by a line charge with an effective linear charge density and for the potential the solution of the linearized Poisson−Boltzmann equation (Debye−Hückel approximation) may be used.[10,11] Nonlinear screening effects within the inner double layers are accounted for by variation of the effective linear charge density. For this purpose, the Debye−Hückel potential is matched to the numerical solution of the nonlinear Poisson−Boltzmann equation for distances from the polyion large compared to the screening length (in the region where the potential drops below kT).

In the Debye−Hückel approximation and including end effects, the second virial coefficient takes the form[12]

$$A_2 = \frac{\pi}{4}L^2 D_{eff}\left(1 + \frac{4D_{eff}}{L}\right) \tag{7}$$

with effective diameter

$$D_{eff} = D_0 + \lambda_D\,(\ln A' + \gamma + \ln 2 - {}^1/_2). \tag{8}$$

Here, γ denotes Euler's constant, $A' = A\,\exp(-D_0/\lambda_D)$ with bare diameter D_0, and A depends on polyion properties.[25] For solutions in excess simple salt with ionic strength ρ_s, the screening length λ_D is given by $\lambda_D{}^{-2} = 8\pi Q\rho_s$ with the Bjerrum length $Q = e^2/\epsilon kT$. Odijk has also proposed an approximation for the third virial coefficient (neglecting end effects)[12]

$$A_3 = \left(\frac{\pi}{4}L^2 D_{eff}\right)^2 \frac{4D_{eff}}{L} \tag{9}$$

which scales as the effective diameter to the third power.

Unfortunately, the theoretical structure factor (with limiting form eq 6) has a rather restricted validity. Flexibility effects are not included, but, as in case of the molecular form function, they are expected to be modest under the present conditions ($L \lesssim 2L_p$ and $qL \gtrsim 5$). More serious is the neglect of high q nonelectroneutral (small) ion fluctuations and interference contributions within

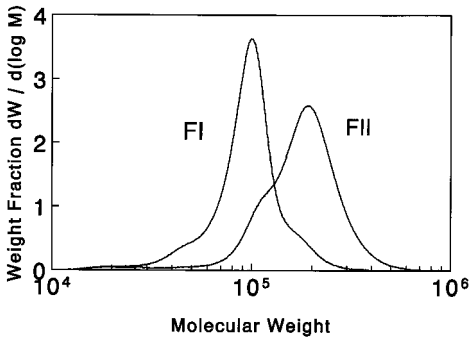

Figure 1. Na−DNA differential molecular weight distribution. The molecular weight characteristics are collected in Table 1.

Table 1. Na−DNA Average Molecular Weight M_w, Polydispersity Ratio M_w/M_n, and Weight Average Contour Length L of SEC Eluents

fraction	M_w	M_w/M_n	L (nm)
FI	104 000	1.14	54
FII	202 000	1.20	104

the excluded volume itself. The theory is valid in the range $q < \lambda_D^{-1}$, i.e., at low values of momentum transfer and/or excess salt conditions, and does not exhibit oscillations at the level of the third virial approximation.[15]

Experimental Section

DNA fragments were obtained by micrococcal nuclease digestion of calf thymus chromatin.[26] After precipitation in cold 2-propanol, the DNA pellet was dried under reduced pressure at room temperature. The DNA was brought to the salt-free sodium form by dissolving it in a 50 mM NaCl, 24 mM EDTA buffer and performing extensive dialysis against water (purified by a Millipore system with conductivity less than 1×10^{-6} Ω^{-1} cm^{-1}). To avoid denaturation, care was taken that the DNA concentration did not drop below 3 mM nucleotides/L. The differential molecular weight distribution was monitored by size exclusion chromatography (SEC) with light scattering detection.[27] The advantage of the isolation procedure is that it yields a large quantity of mononucleosomal DNA, but a typical batch contains approximately 25% lower and higher molecular weight material. Further SEC fractionation resulted in two relatively monodisperse eluent fractions FI−II. Their differential molecular weight distributions are displayed in Figure 1. The average molecular weights, polydispersity, and weight average contour lengths are collected in Table 1. Eluent FI contains mononucleosomal DNA. Fraction FII contains incompletely digested DNA, but with a relatively narrow molecular weight distribution centered about twice the mononucleosomal value. The ratio of the optical absorbencies $A_{260}/A_{280} = 1.9$ shows the material is essentially free of protein.[28] The hypochromic effect at 260 nm confirmed the integrity of the double helix. The material was freeze-dried and the residual water content was determined by IR spectroscopy.

Samples were prepared by dissolving freeze dried Na−DNA in 0.04, 0.2, 1, or 2 M KBr in H_2O. We have used KBr instead of NaCl to minimize an incoherent scattering contribution related to the small ions. The DNA concentrations are 0.05, 0.1, or 0.2 mol of nucleotides/L and are sufficiently low to avoid formation of multimolecular aggregates.[18] All concentrations are determined by weight, using the water content in the freeze-dried material and the Na−DNA partial molar volume of 165 cm^3/mol. The solutions contain a mixed cation, i.e. Na^+ originating from the dissolved DNA material and added K^+. The nucleotide scattering length contrast $\bar{b} = 11.36 \times 10^{-12}$ cm has been calculated using the values reported by Jacrot and according to the calf thymus base composition A:G:C:T:5-methylcytosine = 0.28:0.22:0.21:0.28:0.01.[29] Standard quartz sample containers with 0.1 cm path length were used.

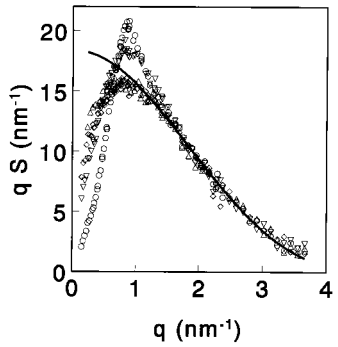

Figure 2. DNA fragment structure function multiplied by momentum transfer in 0.04 (○), 0.2 (▽), 1 (◇), and 2 (△) M KBr (eluent fraction I with most probable contour length 54 nm). The nucleotide concentration is 0.1 M. The solid line denotes the square of the Hankel transform of the radial steplike DNA density with radius $r_p = 0.8$ nm.

Small angle neutron scattering experiments were done with the PAXY and D17 diffractometers, situated on the cold sources of the high neutron flux reactors at the Laboratoire Leon Brillouin (LLB), CEN de Saclay, and Institute von Laue-Langevin (ILL), respectively. The temperature was kept at 293 K. Most samples were measured with the PAXY instrument in three different experimental configurations. In the first and the second configuration, a wavelength of 0.8 nm was selected, and the effective distances between the sample and the planar square multidetector ($S-D$ distance) were 3.2 and 1.2 m, respectively. This allows for a momentum transfer range of 0.1−2.3 nm^{-1}. The counting time per sample or solvent was approximately 7 h. In the third configuration, a wavelength of 0.5 nm was selected with $S-D$ distance of 1.2 m. Here, the momentum transfer ranged from 0.5 to 3.7 nm^{-1}, with a counting time of approximately 4 h/sample. The 0.05 mol of nucleotides/L DNA data were collected with the D17 instrument in two different configurations. The wavelength was fixed at 0.9 nm, and the detector was subsequently placed at 2.9 and 0.8 m from the sample position. These $S-D$ distances allow for a momentum transfer range of 0.1−0.8 and 0.5−2.2 nm^{-1}, respectively. The D17 counting times were 2 h/sample, irrespective of $S-D$ distances. Data correction allowed for sample transmission and detector efficiency. Absolute scattering intensities were obtained by reference to pure water, and the scattering of the pure solvent was subtracted. No additional incoherent scattering correction was performed. It was observed that the reference solvents, i.e., saline solutions without DNA, do not show significant scattering in the present range of momentum transfer. In polyelectrolyte solutions, the scattered intensity often displays an upturn for $q < 0.2$ nm^{-1}.[7,30] This upturn is more or less proportional to the D_2O mole fraction and vanishes in H_2O for $q > 0.08$ nm^{-1}. An explanation can not be given, but under the present experimental conditions the data seem not to be influenced by this effect.

Results and Discussion

Form Function. Figure 2 displays qS of 0.1 M nucleotides/L DNA with a most probable contour length $L = 54$ nm for various excess salt concentrations in the range 0.04−2 M KBr. No plateau value in the qS vs q plot is observed. The absence of rodlike q^{-1} scaling is related to the finite DNA cross section. With increasing salt concentration the peak intensity decreases with a concurrent increase in intensity at longer wavelengths (smaller q values). These effects are due to ionic strength dependent intermolecular interference and will be discussed below. For higher q values the structure functions approach the intrachain function. Flexibility

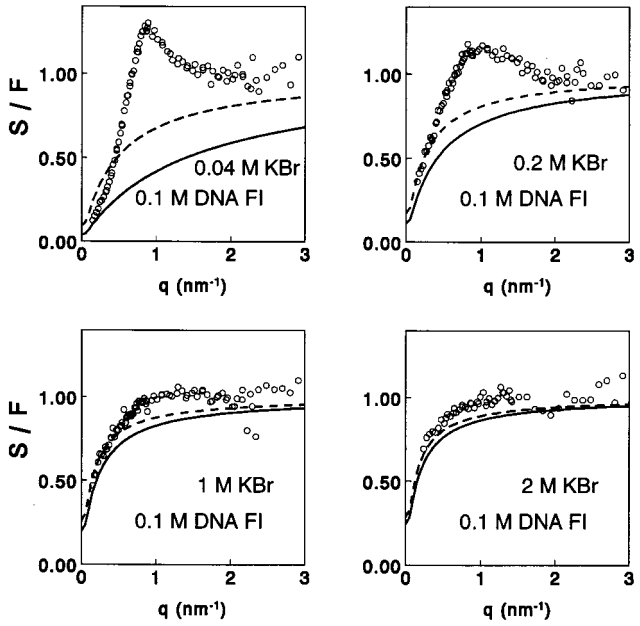

Figure 3. Excess salt dependence of the mononucleosomal DNA structure function divided by the form function of a uniform rod (with $L = 54$ nm, $r_p = 0.8$ nm). The nucleotide concentration is 0.1 M. Dashed lines refer to second virial theory for the structure factor; the solid curves include the contribution of the third virial coefficient.

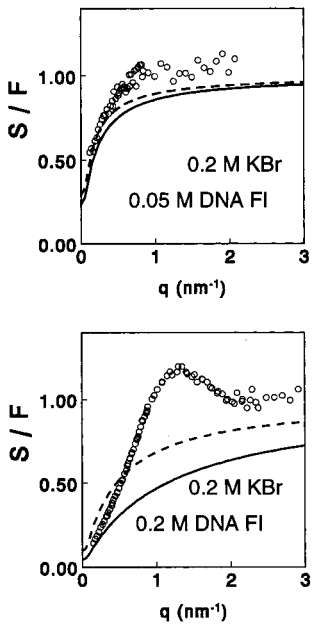

Figure 4. DNA concentration dependence of the structure factor in 0.2 M KBr (mononucleosomal DNA, $L = 54$ nm). The curves are plotted as in Figure 3.

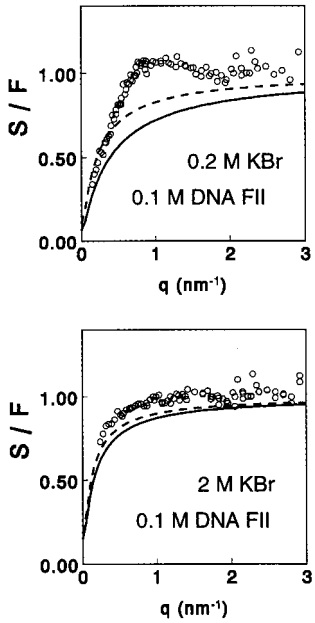

Figure 5. Plot as in Figure 3, but for DNA eluent fraction II (with most probable contour length $L = 104$ nm).

effects on the form function are less than 4% for our lower bound $qL \approx 5$ and become negligible as q is increased.[21] The solid curve in Figure 2 has been drawn according to the limiting form of the rigid rod form function eqs 4 and 5 with radius $r_p = 0.8$ nm and nucleotide (charge) spacing $A = 0.171$ nm. The value of the radius is somewhat less than the outer value of 1 nm, which is related to the relatively open molecular DNA structure and the existence of grooves. As an alternative procedure, the DNA cross section can be described by a Gaussian radial nucleotide profile.[8] Such a profile gives an equally good fit (results not shown), and the radius r_p can be interpreted as a second moment. For the other samples similar scattering behavior is observed (results not shown).

Solution Structure. Effects of intermolecular organization are most clearly demonstrated when the total structure function is divided by the intrachain function. We have used the full theoretical expression of the rigid rod form function (including end effects), together with the parameters for the DNA cross section and nucleotide spacing.[7] However, in the present range $qL \gtrsim 5$ end effects are negligible, and the form function can to a very good approximation be represented by its limiting form, eq 4. With $L \lesssim 2L_p$ and $qL \gtrsim 5$ flexibility effects are modest (<4%), even for our longer fragments with most probable contour length $L = 104$ nm.[21] Figure 3 displays the solution structure $S(q)/F(q)$ of 0.1 M persistence length DNA fragments in 0.04−2 M KBr. The DNA ($L = 54$ nm) concentration dependence in 0.2 M KBr is displayed in Figure 4. Results pertaining to eluent fraction II DNA (with most probable contour length $L = 104$ nm) in 0.2 and 2 M KBr are displayed in Figure 5. The DNA structure factors are similar to those reported for charged rodlike TMV and fd virus solutions, except for the fact that the peak occurs at higher q values due to differences in molecular dimensions.[16]

For lower excess salt and/or higher DNA concentration the solution structure function $S(q)/F(q)$ oscillates about unity and shows a peak at finite wavelength. Our rod number concentrations exceed the overlap concentration L^{-3} by at least an order of magnitude (see Table 2) and the solutions are semidilute. The peak position scales with DNA nucleotide concentration according to $\rho_L^{1/2}$, which is common for (locally) rodlike particles in the semidilute regime.[8,19,31,32] With increasing excess salt concentration the peak shifts to slightly higher q values ($q_m = 0.85$, 1.0, and 1.25 nm^{-1} in 0.04, 0.2, and 1 M KBr, respectively) and its intensity decreases. Eventually, the peak disappears if the salt concentration exceeds 0.2 and 1 M for 0.05 and 0.1 M DNA, respectively. Furthermore, a concurrent peak broadening and intensity increase in the longer wavelength (smaller q) region is observed. Complete suppression of the inter-

Table 2. Nucleotide Concentration, Excess Salt Concentration, Contour Length, Screening Length, Effective DNA Diameter, Scaled Fragment Density, and Second Virial and Third Virial Contributions

C_{DNA} (M)	C_{salt} (M)	L (nm)	λ_D (nm)	D_{eff} (nm)	$\rho_L L^3$	$A_2\rho_L$	$A_3\rho_L^2$
0.1	2.0	54	0.2	2.4	30	1.24	0.20
0.1	1.0	54	0.3	2.7	30	1.43	0.39
0.1	0.2	54	0.7	4.2	30	2.40	1.05
0.1	0.04	54	1.3	7.3	30	4.85	5.36
0.2	0.2	54	0.6	4.1	60	4.69	3.96
0.05	0.2	54	0.7	4.2	15	1.21	0.27
0.1	2.0	104	0.2	2.4	111	2.23	0.39
0.1	0.2	104	0.7	4.2	111	4.11	2.03

molecular contribution is not observed. The structure functions of fragments with different contour lengths, but with equal nucleotide and excess salt concentrations, are remarkably similar.

The peak in the solution structure is due to interference within the excluded volume itself on a length scale on the order of the screening length (at $q \approx \lambda_D^{-1}$, see Table 2). This explains why the peak shifts to slightly higher q values with increasing salt concentration. A theoretical interpretation of the interference contribution requires a full understanding of the pair correlation, taking into account high q (small) ion fluctuations and nonlinear screening effects within the inner double layers. To date no satisfactory theory is available to describe high q polyelectrolyte interference. For longer wavelengths and/or short screening lengths in the range $q < \lambda_D^{-1}$, the scattering can be explained with virial theory and electrostatic interactions in the Debye−Hückel approximation (with renormalized linear charge densities). Accordingly, this theory is expected to be relevant at low values of momentum transfer and/or high excess salt conditions.

Virial Theory. All relevant parameters in the calculation of the virial coefficients are collected in Table 2. Effective diameters D_{eff} (eq 8) are obtained from the nonlinear Poisson−Boltzmann equation for cylindrical polyelectrolytes with excess simple salt. The bare DNA diameter D_0 was set to the conventional value 2 nm. Screening by counterions originating from DNA cannot be neglected and has been estimated according to the condensation concept.[33] The screening lengths in Table 2 are calculated on the basis of the added salt concentration and an uncondensed counterion fraction 0.24. The virial coefficients A_2 and A_3 are calculated according to eqs 7 and 9, respectively, and are also collected in Table 2.[34] The third virial contribution is never negligible and becomes particularly appreciable for solutions with low ionic strength and/or high DNA concentration. It should be noted that the expression for A_3 (eq 9) is approximate only and does not include end effects.

The solution structure functions based on virial theory are displayed in Figures 3−5. Dashed curves refer to the second virial approximation, whereas the solid curves are calculated including the third virial coefficient A_3. For the sake of completeness, we have used the full expression including finite length effects.[7] However, in our experimental range of momentum transfer, the solution structure function is to a very good approximation equal to its limiting form given by eq 6. Flexibility effects on the solution structure are unknown, but, as in case of the form function, they are expected to be modest (<4%) for $L \lesssim 2L_p$ and $qL \gtrsim 5$.[21] The theoretical solution structure function does not show a maximum or any oscillation but reproduces the experimental data for longer wavelengths and/or high excess salt concentration with $q < \lambda_D^{-1}$.

At low values of momentum transfer, the ionic strength, contour length, and concentration dependence of the solution structure is reasonably well predicted by virial theory. As far as the ionic strength and DNA concentration is concerned, this was also observed with static light scattering from similar fragments in the region $qL < 1.8$.[18] Inclusion of A_3 gives a significant improvement, especially for samples with low amount of added salt or higher DNA concentration. For the latter samples the data approach the thermodynamic $q \rightarrow 0$ limit, but for solutions with higher salinity the theoretical solution structure shows a steep decrease just below our lower limit $q \lesssim 0.1$ nm^{-1}. In case of high excess salt concentration (1 and 2 M) the condition $q < \lambda_D^{-1}$ is satisfied in the whole experimental q range. As can be seen in Figures 3 and 5, for these salinity's the data still deviate from theory despite the fact that the correlation peak is (almost) completely suppressed. These deviations can be explained by the fact that we have optimized the DNA radius under the neglect of the interference contribution for high q values. Accordingly, the optimization procedure forces the solution structure function to unity at high q and the observed deviations are probably insignificant.

Conclusions

For short DNA fragments immersed in salt solutions both the limiting low q behavior and the correlation peak of the solution structure function are fairly sensitive to ionic strength and DNA volume fraction. Under the present experimental conditions, the effects of the DNA contour length are moderate. The scattering behavior in front of the correlation peak at lower values of momentum transfer and/or high supporting electrolyte concentration can be rationalized with virial theory up to and including the third coefficient and screened electrostatics. Virial theory is strictly valid for wavelengths exceeding the screening length and, accordingly, does not predict the oscillations and/or correlation peak displayed by strongly interacting systems at higher q values. In added salt concentrations exceeding, e.g., 1 M, the correlation peak is almost completely suppressed and neutral polymer behavior is recovered. The present data can also be compared with other theoretical approaches, such as liquid-state integral theory, as well as numerical simulation.[35] However, for a complete description of the solution structure at higher values of momentum transfer it is mandatory to include fluctuations and interactions within the excluded volume itself.

Acknowledgment. We thank A. Lapp, S. Egelhaaf, W. Jesse, J. A. P. P. van Dijk, and M. E. Kuil for support and assistance with SANS experiments. T. Odijk, A. Yethiraj, and C.-Y. Shew are gratefully acknowledged for stimulating discussions. We acknowledge the Laboratoire Léon Brillouin and Institut Laue-Langevin in providing the neutron research facilities.

References and Notes

(1) Katchalsky, A. *Pure Appl. Chem.* **1971**, *26*, 327.
(2) Onsager, L. *Ann. N.Y. Acad. Sci.* **1949**, *51*, 627.
(3) Odijk, T. *J. Polym. Phys. Ed.* **1977**, *15*, 477.
(4) Kassapidou, K.; Heenan, R. K.; Jesse, W.; Kuil, M. E.; van der Maarel, J. R. C. *Macromolecules* **1995**, *28*, 3230.
(5) Kassapidou, K.; Jesse, W.; van Dijk, J. A. P. P.; van der Maarel, J. R. C. *Biopolymers* **1998**, *46*, 31.

(6) Kassapidou, K.; van der Maarel, J. R. C. *Eur. Phys. J., B* **1998**, *3*, 471.
(7) van der Maarel, J. R. C.; Groot, L. C. A.; Mandel, M.; Jesse, W.; Jannink, G.; Rodriguez, V. *J. Phys. II Fr.* **1992**, *2*, 109.
(8) Kassapidou, K.; Jesse, W.; Kuil, M. E.; Lapp, A.; Egelhaaf, S.; van der Maarel, J. R. C. *Macromolecules* **1997**, *30*, 2671.
(9) Bhuiyan, L. B.; Outhwaite, C. W.; van der Maarel, J. R. C. *Physica A* **1996**, *231*, 295.
(10) Brenner, S.; Parsegian, V. A. *Biophys. J.* **1974**, *14*, 327.
(11) Fixman, M.; Skolnick, J. *Macromolecules* **1978**, *11*, 863.
(12) Odijk, T. *J. Chem. Phys.* **1990**, *93*, 5172.
(13) Maeda, T. *Macromolecules* **1991**, *24*, 2740.
(14) Odijk, T. *Laser Light Scattering in Biochemistry*; Harding, S. E., Satella, D. B., Bloomfield, V. A., Eds.; Royal Society of London: London, 1992.
(15) Odijk, T. *Light Scattering, Principles and Development*; Brown, W., Ed.; Oxford University Press: Oxford, England, 1996.
(16) Maier, E. E.; Krause, R.; Deggelmann, M.; Hagenbüchle, M.; Weber, R.; Fraden, S. *Macromolecules* **1992**, *25*, 1125, and references cited therein.
(17) Nicolai, T.; Mandel, M. *Macromolecules* **1989**, *22*, 438.
(18) Wissenburg, P.; Odijk, T.; Cirkel, P.; Mandel, M. *Macromolecules* **1995**, *28*, 2315.
(19) Wang, L.; Bloomfield, V. A. *Macromolecules* **1991**, *24*, 5791.
(20) Jannink, G.; van der Maarel, J. R. C. *Biophys. Chem.* **1991**, *41*, 15.
(21) Norisuye, T.; Murakama, H.; Fujita, H. *Macromolecules* **1978**, *11*, 966.
(22) Shimada, T.; Doi, M.; Okano, K. *J. Chem. Phys.* **1988**, *88*, 2815.
(23) van der Schoot, P.; Odijk, T. *Macromolecules* **1990**, *23*, 4181.
(24) Maeda, T. *Macromolecules* **1989**, *22*, 1881.
(25) Stroobants, A.; Lekkerkerker, H. N. W.; Odijk, T. *Macromolecules* **1986**, *19*, 2232.
(26) Wang, L.; Ferrari, M.; Bloomfield, V. A. *BioTechniques* **1990**, *9*, 24.
(27) Nicolai, T.; van Dijk, L.; van Dijk, J. A. P. P.; Smit, J. A. M. *J. Chromatogr.* **1987**, *389*, 286.
(28) Liebe, D. C.; Stuehr, J. E. *Biopolymers* **1972**, *11*, 167.
(29) Jacrot, B. *Rep. Prog. Phys.* **1976**, *39*, 911.
(30) van der Maarel, J. R. C.; Groot, L. C. A.; Hollander, J. G.; Jesse, W.; Kuil, M. E.; Leyte, J. C.; Leyte-Zuiderweg, L. H.; Mandel, M.; Cotton, J. P.; Jannink, G.; Lapp, A.; Farago, B. *Macromolecules* **1993**, *26*, 7295.
(31) Groot, L. C. A.; Kuil, M. E.; Leyte, J. C.; van der Maarel, J. R. C.; Heenan, R. K.; King, S. M.; Jannink, G. *Liq. Cryst.* **1994**, *17*, 263.
(32) Nierlich, M.; Williams, C. E.; Boué, F.; Cotton, J.-P.; Daoud, M.; Farnoux, B.; Jannink, G.; Picot, G.; Moan, M.; Wolff, C.; Rinaudo, M.; de Gennes, P. G. *J. Phys. Fr.* **1979**, *40*, 701.
(33) Manning, G. S. *J. Chem. Phys.* **1969**, *51*, 924.
(34) As far as we are aware, polydispersity effects on the scattering behavior of rodlike polymer solutions are unknown, except for forward scattering ($q \rightarrow 0$) in the second virial approximation (and under the neglect of end group effects). Under these conditions, A_2 is *not* a simple number average, as one might intuitively expect from the virial expansion of the equation of state. Inserting the number-averaged contour length would lead to a severe underestimation of the virial coefficients. We have used the molecular weight average contour length instead, since this corresponds with the most probable contour length (see Figure 1).
(35) Yethiraj, A.; Shew, C.-Y. *Phys. Rev. Lett.* **1996**, *77*, 3937.

MA9805710